*Journal of Zhejiang University-SCIENCE A (Applied Physics & Engineering) in press*
www.jzus.zju.edu.cn; www.springer.com/journal/11582
E-mail: jzus_a@zju.edu.cn

**Research Article**

https://doi.org/10.1631/jzus.A2400427

# Probabilistic analysis of settlement characteristics induced by shield tunnelling in sandy cobble strata considering spatial variability

Fan WANG[1], Pengfei LI[2]✉, Xiuli DU[2], Jianjun MA[1], Lin WANG[1]

[1] *School of Civil Engineering and Architecture, Henan University of Science and Technology, Luoyang 471023, China*
[2] *Key Laboratory of Urban Security and Disaster Engineering, Ministry of Education, Beijing University of Technology, Beijing 100124, China*

**Abstract:** Sandy cobble soil exhibits pronounced heterogeneity. The assessment of the uncertainty surrounding its properties is crucial for the analysis of settlement characteristics resulting from volume loss during shield tunnelling. In this study, a series of probabilistic analyses of surface and subsurface settlements was conducted considering the spatial variability of the friction angle and reference stiffness modulus, under different volumetric block proportions (VBP) and tunnel volume loss rates ($\eta_t$). The non-intrusive random finite difference method was used to investigate the probabilistic characteristics of maximum surface settlement, width of subsurface settlement trough, subsurface maximum settlement and subsurface soil volume loss rate through Monte Carlo simulations. Additionally, a comparison between stochastic and deterministic analysis results is presented to underscore the significance of probabilistic analysis. Parametric analyses were subsequently conducted to investigate the impacts of the key input parameters in random fields on the settlement characteristics. The results indicate that scenarios with higher *VBP* or greater $\eta_t$ result in a higher dispersion of stochastic analysis results. Neglecting the spatial variability of soil properties and relying solely on the mean values of material parameters for deterministic analysis may result in an underestimation of surface and subsurface settlements. From a probabilistic perspective, deterministic analysis alone may prove inadequate in accurately capturing the volumetric deformation mode of the soil above the tunnel crown, potentially affecting the prediction of subsurface settlement.

**Key words:** Shield tunnels; Sandy cobble strata; Settlement characteristics; Spatial variability; Probabilistic analysis

## 1 Introduction

Sandy cobble soil represents a distinctive geological formation, composed mainly of cobbles, gravels, sand and a minor proportion of clay (Wang et al., 2023). Numerous shield tunnels have been constructed within sandy cobble strata in various Chinese cities including Beijing, Chengdu, and Lanzhou. The issue of ground movement induced by shield tunnelling in sandy cobble strata is always a hot topic and arouses extensive concern. Di et al. (2022) conducted a series of model tests and numerical analyses to investigate the progressive settlement induced by the instability of the face of tunnels in sandy cobble strata. Cao et al. (2019) found that the longitudinal surface settlement of tunnel boring machine (TBM) tunneling in sandy cobble strata can be well predicted by the Attewell formula. Wang et al. (2024, 2023a) proposed methods for predicting subsurface and surface settlements induced by shield tunnels in sandy cobble strata, respectively. Based on numerical simulation and field data, Li and Geng (2024) studied the deformation response of an old building under-crossed by overlapping tunnels in sandy cobble strata. The settlement characteristics of twin tunnels in sandy cobble strata were also revealed by some researchers through numerical analysis (Hao et al., 2021; He et al., 2012). These studies considered sandy cobble strata as a homogeneous material and the material properties were assumed to be constant when performing numerical analysis. However, the particle sizes of sandy cobble strata vary from small-sized sands to large-sized cobbles, showing noteworthy heterogeneity. Furthermore, the spatial location of cobbles distributes randomly. Thus, the soil properties at different locations are bound to

✉ Pengfei LI, lpf@bjut.edu.cn
Pengfei LI, https://orcid.org/0000-0002-4996-368X

Received Aug. 30, 2024; Revision accepted Oct. 17, 2024; Crosschecked

© Zhejiang University Press 2024

show significant spatial variability.

Several researchers have used the random variable method to perform probabilistic analyses of the ground movements (Mollon et al., 2013) and face stability (Mollon et al., 2011, 2009a, 2009b) of tunnels. This method treats the geomaterials as homogeneous bodies and considers material parameters as purely random variables. The statistical mean, variance, and coefficient of variation of material parameters within the whole research area are used to represent the overall probabilistic characteristics, failing to consider the differences in material parameters between different locations in space (Zhang et al., 2022) and overestimating the failure probability (Cheng et al., 2019a). In reality, the spatial variability of geomaterials not only shows the characteristics of heterogeneity and randomness, but also spatial correlation of soil properties at different locations.

Vanmarcke (1977) pioneered the use of random field theory to characterize the inherent spatial variability of geomaterials and proposed the concept of scale of fluctuation to reflect the correlation of soil properties. Random field theory has been widely used in the field of tunnelling and underground engineering when considering the spatial variability of geomaterials. Based on the existing failure mechanism of a tunnel face, some researchers have used the random limit analysis method (Cheng et al., 2019; Cheng et al., 2019b; Li et al., 2021) and the sparse polynomial chaos expansion method (Li et al., 2022; Pan & Dias, 2017) to study the stability of a tunnel face. Using numerical analyses, several researchers combined random field theory and finite element/difference method to investigate the probabilistic characteristics of tunnel deformation (Huang et al., 2017; Lü et al., 2018; Wu et al., 2021; Zhang et al., 2021) and assess the stability of tunnels (Ali et al., 2017; Pan et al., 2019; Pandit and Sivakumar Babu, 2021; Wu et al., 2021). The random finite element/difference method is a popular approach to evaluate the effect of inherent spatial variability of soil properties on tunnelling-induced ground movements (Cheng et al., 2019c; Wu et al., 2024; Zhang et al., 2024). However, its application in sandy cobble strata has rarely been reported. Although Zhang et al. (2023) adopted the random finite difference method to simulate the deformation of a tunnel in sandy pebble soil, the purpose was to propose a deep learning method for reliability analysis of tunnel convergence other than the probabilistic analysis of ground settlement. Due to the heterogeneity and randomness of sandy cobble soil, it is necessary to investigate the probabilistic characteristics of tunnelling-induced settlement considering the inherent spatial variability of soil properties.

In our previous research (Wang et al., 2024), considering the ground loss variation with depth, we performed a series of deterministic numerical analyses under different cover depth ratios and cobble contents to discuss the variation of surface and subsurface settlement characteristics induced by volume loss of shield tunnelling in sandy cobble strata. In this study, from a probabilistic perspective, a series of non-intrusive random finite difference numerical analyses under different cobble contents and tunnel volume loss rates was performed to investigate the probabilistic characteristics of surface and subsurface settlements induced by volume loss of shield tunnelling in sandy cobble strata through Monte Carlo simulations. Then, comparisons between the results of deterministic and stochastic analyses were made to emphasize the significance of stochastic analysis to tunnelling-induced settlement in sandy cobble strata. Finally, sensitivity analyses were conducted to discuss the effects of the key input parameters in random fields on the stochastic analysis results.

## 2 Random finite difference numerical analysis

Considering the spatial variability of the soil properties of sandy cobble soil, the non-intrusive random finite difference method combining random field theory, finite difference method, and Monte Carlo simulation was adopted to investigate the probabilistic characteristics of surface and subsurface settlements induced by tunnel volume loss under different volumetric block proportions (VBPs, i.e., cobble contents) and tunnel volume loss rates ($\eta_t$). The so-called non-intrusive random analysis method refers to a process in numerical simulation where the random field modeling is separate and not coupled with finite difference numerical computations (Jiang et al., 2014). All the numerical simulations were performed using the finite difference program

FLAC$^{3D}$ (Itasca 2017).

### 2.1 Numerical modeling

A circular shield tunnel embedded in a spatially variable sandy cobble soil was considered here with a common diameter $D = 6$ m and the cover depth $C = 12$ m (i.e., $C/D = 2.0$) for urban subway tunnels (Fig. 1). To avoid boundary effects, the numerical model was set as 60 m in width and 36 m in depth. The thickness was set as 0.1 m to simulate the plane strain condition. The lateral boundaries of the model were fixed in the normal direction, while the bottom boundary was fixed in both the horizontal and vertical directions. The ground surface was free. The multi-scale numerical analysis method was used here to improve computational efficiency. The region close to the tunnel circumference, which is significantly affected by the excavation, was considered the "region of interest". The sizes of this region were set as 30 m in width and 21 m in depth. The elements in the region of interest were assigned material parameters generated by the random field modeling, while those in other regions were assigned the mean value of material parameters. To ensure computational accuracy, it is important that the element sizes in the region of interest should conform to the principles related to element sizes in random fields (Ching and Phoon, 2013). The tunnel volume loss ($V_t$) induced by the gap between the excavation profile and external boundary of lining was simulated by applying a displacement boundary condition around the tunnel circumference (Wang et al., 2024; Zhang et al., 2016). Considering the classical non-uniform deformation pattern of the tunnel wall, the relationship between the maximum gap ($g_{max}$) at the tunnel crown and the tunnel volume loss rate ($\eta_t$) is expressed by:

$$g_{max} = 2(R - r) = 2r\left(\sqrt{1+\eta_t} - 1\right) \tag{1}$$

where $R$ and $r$ represent the radii of the excavation profile and the external boundary of the lining, respectively.

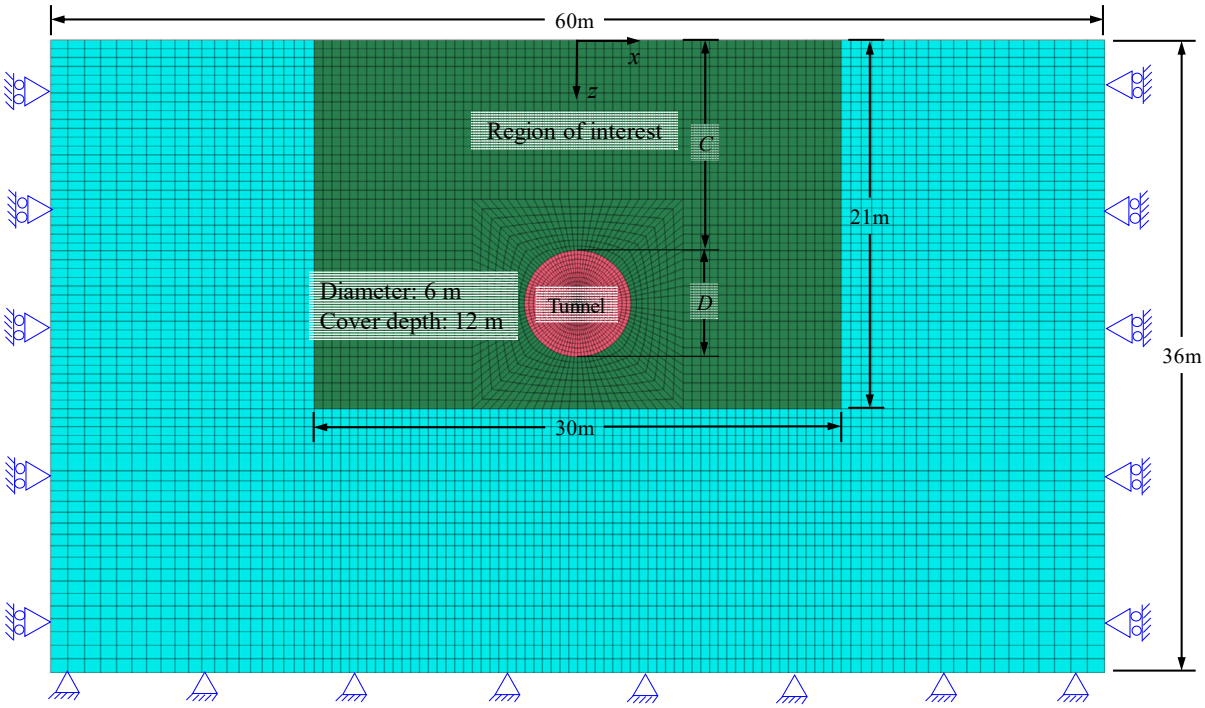


**Fig. 1 Numerical model of non-intrusive stochastic analysis**

Due to the strain-hardening characteristic of sandy cobble soil, the Hardening-Soil model proposed by Schanz et al. (1999) was adopted to describe the overall stress-strain behavior (Wang et al., 2024). The volumetric block proportion (VBP) of sandy cobble soil has a significant effect on the overall mechanical behavior. Here, the cases of VBP = 30%, 50%, and 70%, corresponding to low, medium, and

high VBPs, were considered. The material parameters for different VBPs are shown in Table S1 of the electronic supplementary materials (ESM). The calibration of material parameters is described in Section S1 of the ESM. When performing random finite difference numerical simulation, only the spatial variability of the reference secant modulus ($E_{50}^{\mathrm{ref}}$) and friction angle ($\varphi$) were considered due to their significance on the ground settlement. Other parameters were assumed to be deterministic.

## 2.2 Random field modeling of material parameters

Considering the spatial variability of the reference stiffness modulus ($E_{50}^{\mathrm{ref}}$) and friction angle ($\varphi$), input parameters of random field modeling included the mean ($\mu_E$ and $\mu_\varphi$), coefficient of variation ($\mathrm{COV}_E$ and $\mathrm{COV}_\varphi$), horizontal and vertical scales of fluctuation ($\delta_\mathrm{h}$ and $\delta_\mathrm{v}$) and cross-correlation coefficient ($\rho_{\varphi,E}$) of the material parameters. In general, input parameters should be obtained by statistical analysis based on extensive field monitoring data. However, in geotechnical engineering, field monitoring data are often limited and not sufficient to obtain accurate values of each input parameter. To facilitate the comparison between deterministic and stochastic results, $\mu_E$ and $\mu_\varphi$ were taken from Table S1 in the ESM. Other input parameters, except for $\mu_E$ and $\mu_\varphi$, were provided by referring to the statistical results from the literature (Cheng et al., 2019a, 2019c; Wu et al., 2021; Zhang et al., 2021), as shown in Table 1. The effects of these key input parameters will be discussed in section 4.

**Table 1 Values of input parameters of random field modeling under different *VBP*s**

| VBP/% | $\mu_E$/MPa | $\mu_\varphi$/° | $\mathrm{COV}_E$ | $\mathrm{COV}_\varphi$ | $\delta_\mathrm{h}$/m | $\delta_\mathrm{v}$/m | $\rho_{\varphi,E}$ |
|---|---|---|---|---|---|---|---|
| 30 | 25 | 27.57 | | | | | |
| 50 | 40 | 34.95 | **0.1**, 0.2, 0.3, 0.4, 0.5 | 0.05, **0.1**, 0.15, 0.2 | 10, 20, 30, **40**, 50, 60 | 1, 2, 3, **4**, 5, 6 | **0**, 0.25, 0.5, 0.75 |
| 70 | 70 | 49 | | | | | |

Autocorrelation functions are crucial for characterizing the degree of correlation between points in a random field. Exponential and Gaussian autocorrelation functions are two popular functions used in geotechnical engineering (Chen et al., 2019; Deng et al., 2022; Jiang et al., 2014, 2022; Li et al., 2021; Pan et al., 2019; Wu et al., 2021, 2024; Zhang et al., 2024). Random fields that are formulated using the Gaussian autocorrelation function tend to show superior properties in terms of stationarity and continuity. Moreover, fewer truncation terms are required to achieve the desired level of discreteness (Li et al., 2015). Therefore, the following Gaussian autocorrelation function was used:

$$\rho\left(\tau_x,\tau_y\right)=\exp\left[-\pi\left(\frac{\tau_x^2}{\delta_\mathrm{h}^2}+\frac{\tau_y^2}{\delta_\mathrm{v}^2}\right)\right] \tag{2}$$

where $\tau_x$ and $\tau_y$ are the distances between points in the horizontal and vertical directions, respectively.

The Karhunen-Loève expansion method (Huang et al., 2001) was used to discretize the random field, as shown in Section S2 of the ESM. Since soil parameters cannot be negative, the lognormal distribution is generally used to characterize spatial variability (Huang et al., 2017). Furthermore, it is assumed that there is a certain degree of cross-correlation between $E_{50}^{\mathrm{ref}}$ and $\varphi$. $\rho_{\varphi,E}$ denotes the cross-correlation coefficient. In this case, the issue involves cross-correlated non-Gaussian random field modeling. Details of the process are given by Jiang et al. (2014).

## 2.3 Implementation procedure

The random finite difference numerical analysis of surface and subsurface settlement characteristics was performed based on the Monte Carlo strategy. The flowchart is shown in Fig. 2 and the main implementation procedure was as follows:

(1) Construct a multi-scale numerical model for shield tunnels in sandy cobble strata. Extract the centroid coordinates of each element in the region of interest using the Python code.

(2) Determine the input parameters in a random field including the mean, coefficient of variation, scale of fluctuation, and cross-correlation coefficient. Select the autocorrelation function and distribution function.

(3) Perform the Latin Hypercube Sampling in

the independent standard normal space using the MATLAB code. Generate the random field of material parameters through the Karhunen-Loève series expansion method.

(4) Substitute the extracted centroid coordinates and obtain the values of material parameters for each element. Repeat the sampling $N$ times to achieve $N$ realizations of the random field and obtain $N$ sets of values corresponding to each element.

(5) Assign the parameter values generated by the random field to the corresponding element of the numerical model using Python code in FLAC$^{3D}$. The representation in FLAC$^{3D}$ of random field modeling for $E_{50}^{ref}$ and $\varphi$ when VBP = 50% is shown in Fig. S1 of the ESM. Perform the finite difference numerical analysis of tunnelling-induced surface and subsurface settlements. Extract the data of settlement.

(6) Repeat steps (3)~(5) above $N$ times and extract the data of settlement in batches.

(7) Conduct probabilistic analysis of settlement characteristics using Monte Carlo simulations.

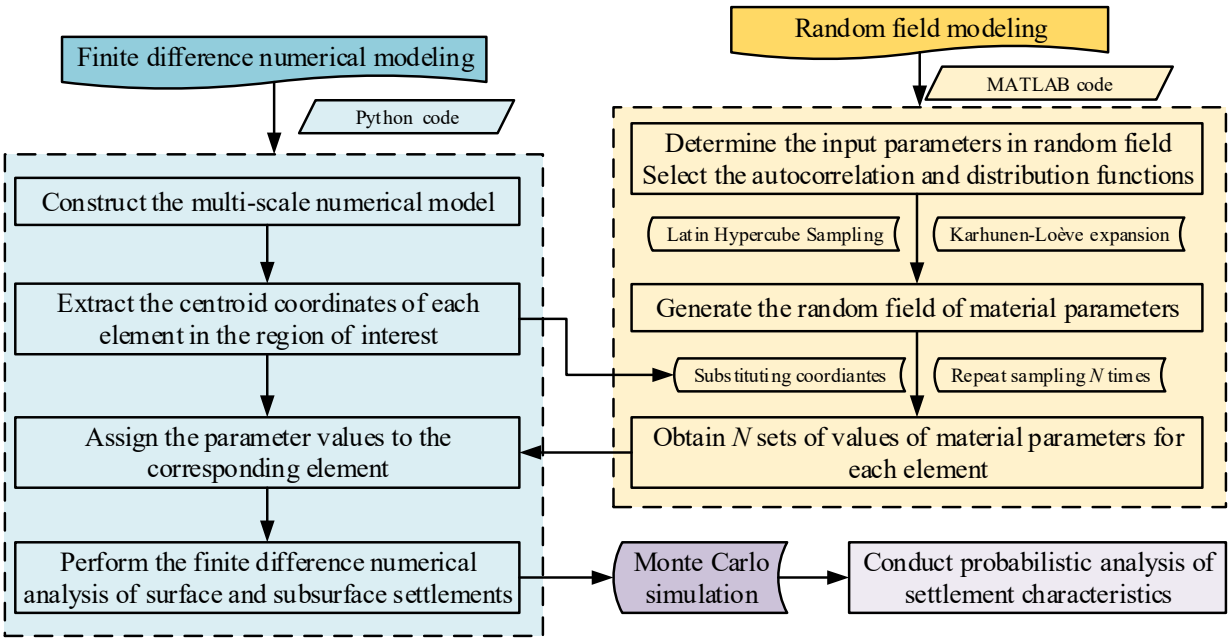


**Fig. 2 Flowchart of random finite difference numerical analysis**

## 2.4 Number of Monte Carlo simulations

When performing probabilistic analysis of settlement characteristics, the number of Monte Carlo simulations should be determined first to ensure results converge and to improve computational efficiency. Taking the case of VBP = 30% as an example, the variation of the mean value and coefficient of variation of the maximum surface settlement against the running number $N$ through 1000 numerical simulations are as shown in Fig. 3. The converged results of the mean and coefficient of variation were achieved when the running number $N$ reached 500. Therefore, $N$ = 500 was taken as a sufficient number of Monte Carlo simulations for the subsequent random finite difference numerical simulations.

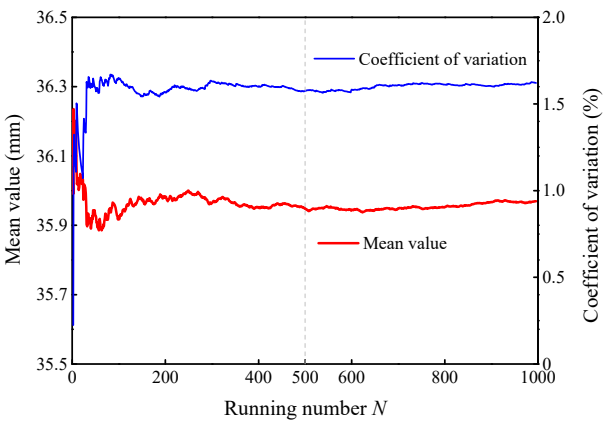


**Fig. 3 Variation of the mean and coefficient of variation of maximum surface settlement against the running number *N***

## 3 Results and comparisons

In this section, probabilistic analyses of surface and subsurface settlements are described for different volumetric block proportions (VBP = 30%, 50%, and 70%) and tunnel volume loss rates ($\eta_t$ = 0.5% and 4.0%). The mean values (i.e., $\mu_E$ and $\mu_\varphi$) were taken from Table S1 in the ESM, while other input parameters in the random field were as follows: $COV_E = COV_\varphi = 0.1$, $\rho_{\varphi,E} = 0$, $\delta_h = 40$ m, and $\delta_v = 4$ m. In addition, the results of stochastic and deterministic analyses were compared to emphasize the significance of probabilistic analysis.

### 3.1 Surface settlement

The probability histograms of maximum surface settlement $S_{max}$ obtained by the stochastic analysis are shown in Fig. 4. The deterministic analysis results are also given for comparison. Regardless of VBP and $\eta_t$, all the stochastic analysis results could be fitted by the probability density curves following the lognormal distribution with the goodness of fit exceeding 90%. As the VBP increases or the $\eta_t$ decreases, the mean ($\mu_s$) of $S_{max}$ by the stochastic analysis tends to be smaller, aligning with the patterns observed in deterministic analysis. However, the stochastic analysis results exhibit a certain level of variability, as shown in Fig. S2 of the ESM. As the VBP or $\eta_t$ increases, the coefficient of variation ($COV_s$) of $S_{max}$ by the stochastic analysis also increases, indicating a higher dispersion. Moreover, scenarios with lower VBP or lower $\eta_t$ tend to a higher probability of the results of stochastic analysis exceeding those of the deterministic analysis.

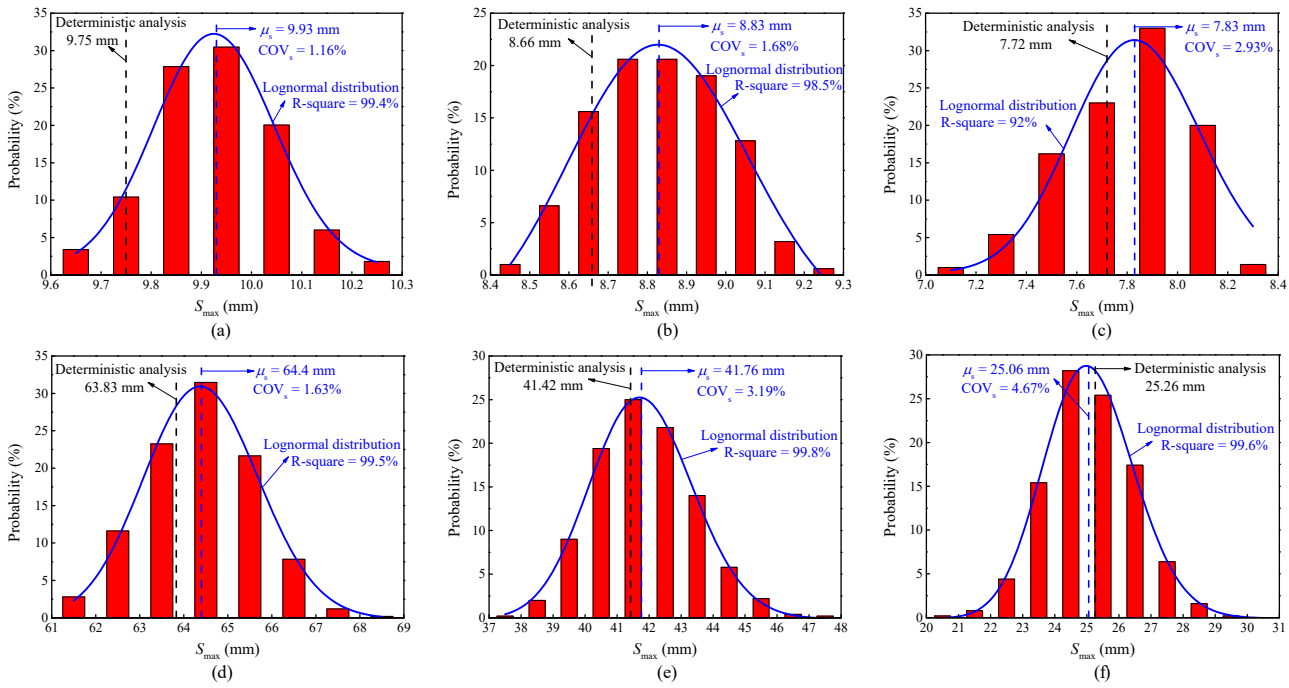


**Fig. 4 Probability histograms of the maximum surface settlement obtained by stochastic analysis: (a)VBP = 30%, $\eta_t$ = 0.5%; (b) VBP = 50%, $\eta_t$ = 0.5%; (c) VBP = 70%, $\eta_t$ = 0.5%; (d) VBP = 30%, $\eta_t$ = 4.0%; (e) VBP = 50%, $\eta_t$ = 4.0%; (f) VBP = 70%, $\eta_t$ = 4.0%**

Fig. 5 depicts the cumulative probability distribution curves of the maximum surface settlement $S_{max}$ obtained by the stochastic analysis exceeding the allowable value $S_{max}^*$. The dashed line represents the deterministic analysis results $S_{max}^d$, and the intersection of the dashed and solid lines gives the probability of $S_{max} > S_{max}^*$. It is evident that the higher the VBP or the lower the $\eta_t$, the lower the probability of $S_{max} > S_{max}^d$. If $S_{max}^* = 20$ mm, then the probability of $S_{max} > S_{max}^*$ is zero when $\eta_t$ = 0.5%, and it reaches 100% when $\eta_t$ = 4.0%. This indicates that for practical engineering, it is crucial to strictly control the quality of backfill grouting to minimize the tunnel volume loss, thereby controlling surface settlement. Moreover, from Fig. 5, when $\eta_t$ = 0.5%, the probabilities of $S_{max} > S_{max}^d$ are 63.76%, 83.62%, and 92.22% for

VBP = 30%, 50%, and 70%, respectively. When $\eta_t$ = 4.0%, the probabilities are 44.38%, 59.24%, and 67.36%, respectively. Namely, the lower the VBP or the lower the $\eta_t$, the higher the probability of $S_{max} > S_{max}^{d}$ (the same result can also be found from Fig. 4). In this case, it is more likely the surface settlement will be underestimated if the deterministic analysis is conducted using only the mean values of material parameters and neglecting the spatial variability of soil properties.

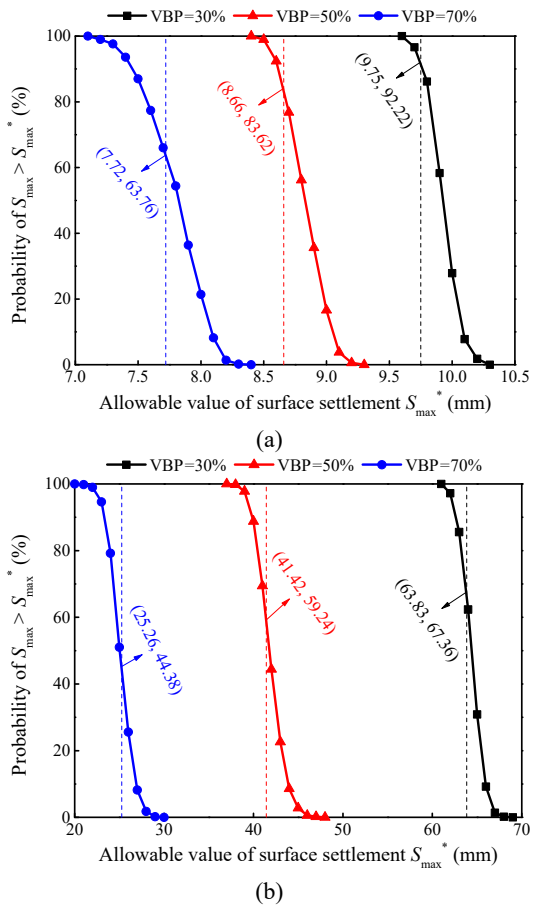


**Fig. 5 Cumulative distribution curves of maximum surface settlements exceeding the allowable values: (a)$\eta_t$ = 0.5%; (b) $\eta_t$ = 4.0%**

## 3.2 Subsurface settlement

### 3.2.1 Width of subsurface settlement trough

The comparison between the stochastic and deterministic analysis results of the normalized subsurface settlement trough width $i(z)/z_0$ with depth $z/z_0$ when $\eta_t$ = 0.5% and 4.0% is presented in Fig. 6. $z_0$ represents the depth of the tunnel centerline. The stochastic analysis results fluctuate around the mean. Overall, for the same VBP, the higher the $\eta_t$, the smaller the stochastic analysis results, which is consistent with the deterministic analysis results. The deterministic analysis results, which were obtained using the mean values of material parameters, are not significantly different from the mean of the stochastic analysis results. However, the stochastic analysis results exhibit dispersion.

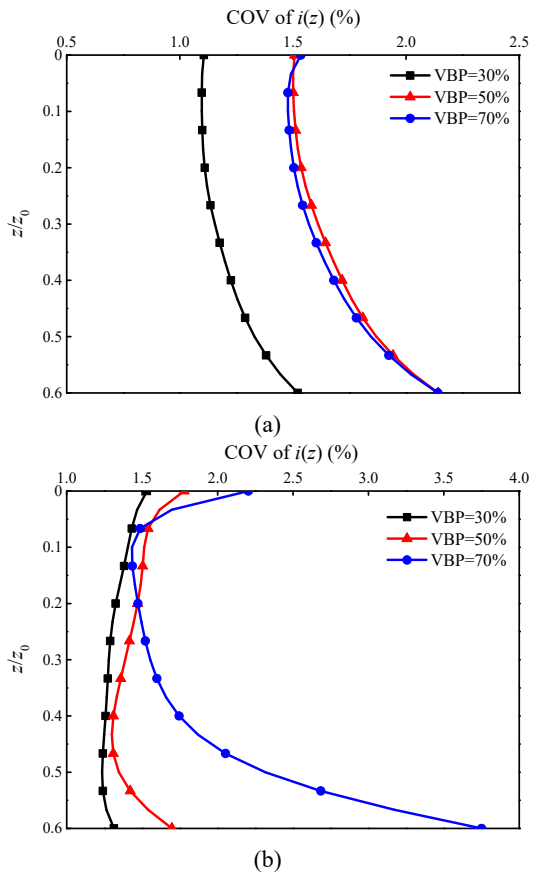


**Fig. 7 COV of stochastic analysis results for subsurface settlement trough width: (a)$\eta_t$ = 0.5%; (b) $\eta_t$ = 4.0%**

The variation of the coefficient of variation (COV) of the stochastic analysis results with depth is shown in Fig. 7. The COV varies greatly at different depths: as the depth increases, the COV generally shows a trend of first decreasing and then increasing. When $\eta_t$ = 0.5%, the COV at the same depth does not differ significantly for the cases of *VBP* = 50% and 70%, and both are greater than the COV for the case of VBP = 30%. When $\eta_t$ = 4.0%, near the ground surface and near the tunnel crown, the COV at the same depth increases with increasing VBP.

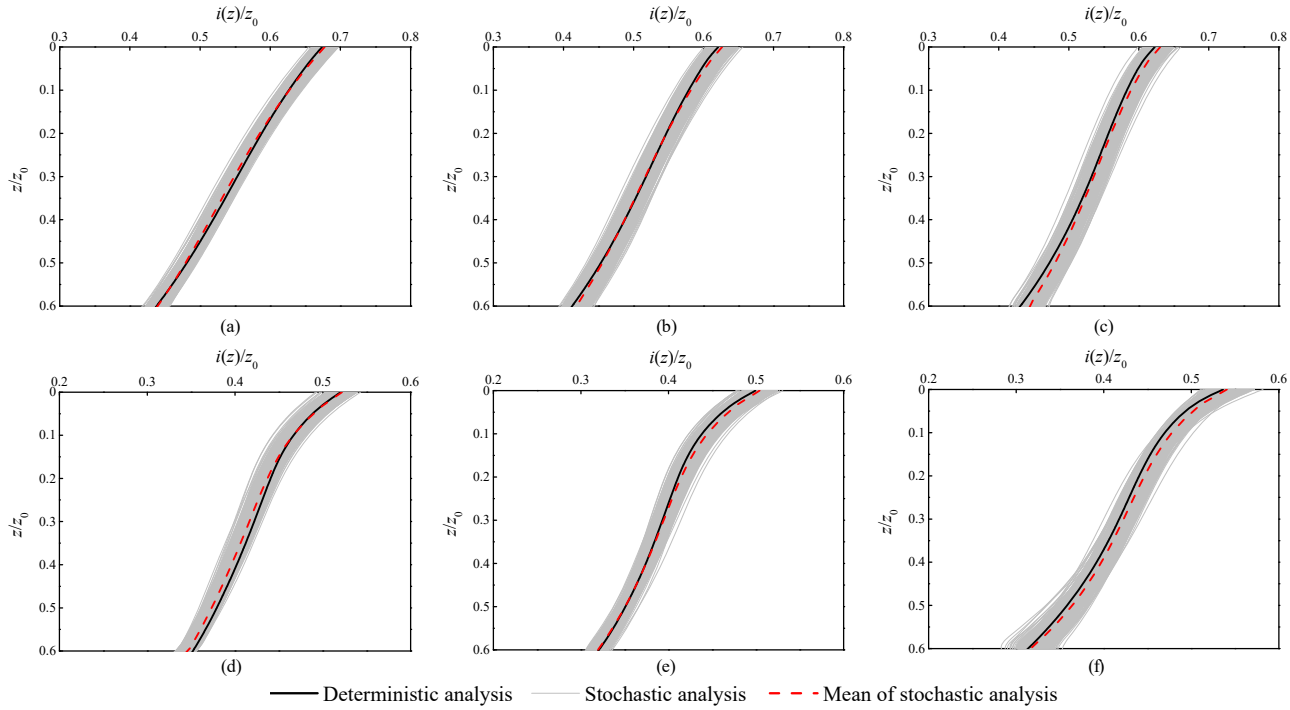


**Fig. 6 Comparison of normalized subsurface settlement trough width between stochastic analysis and deterministic analysis: (a)VBP = 30%, $\eta_t$ = 0.5%; (b) VBP = 50%, $\eta_t$ = 0.5%; (c) VBP = 70%, $\eta_t$ = 0.5%; (d) VBP = 30%, $\eta_t$ = 4.0%; (e) VBP = 50%, $\eta_t$ = 4.0%; (f) VBP = 70%, $\eta_t$ = 4.0%**

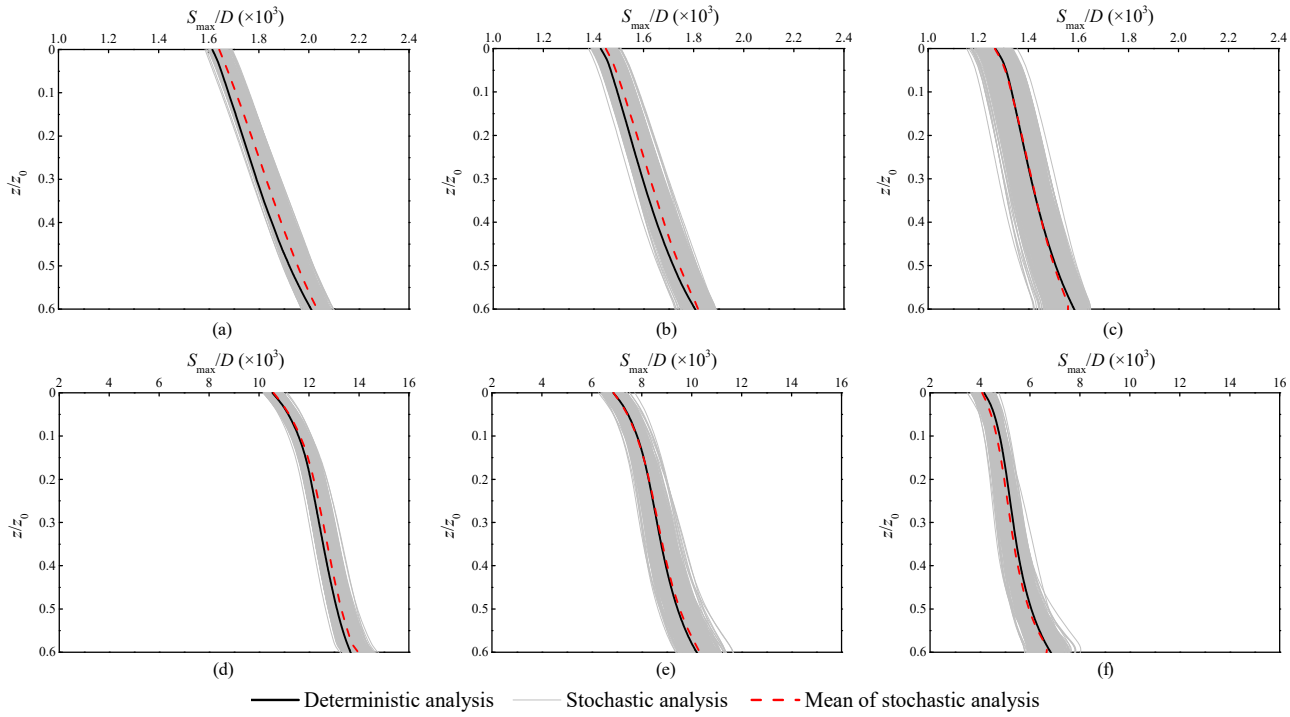


**Fig. 8 Comparison of normalized subsurface maximum settlement between stochastic analysis and deterministic analysis: (a)VBP = 30%, $\eta_t$ = 0.5%; (b) VBP = 50%, $\eta_t$ = 0.5%; (c) VBP = 70%, $\eta_t$ = 0.5%; (d) VBP = 30%, $\eta_t$ = 4.0%; (e) VBP = 50%, $\eta_t$ = 4.0%; (f) VBP = 70%, $\eta_t$ = 4.0%**

### 3.2.2 Subsurface maximum settlement

Fig. 8 compares the results from stochastic

analysis and deterministic analysis of the normalized maximum surface settlement $S_{max}/D$ with depth $z/z_0$ when $\eta_t$ = 0.5% and 4.0%. The higher the VBP or the smaller the $\eta_t$, the smaller the stochastic analysis results. Fig. 8 also reveals that the probability of the stochastic analysis results exceeding the deterministic analysis results is higher for the case of a lower VBP or lower $\eta_t$. This indicates that for a lower VBP or lower $\eta_t$, neglecting the spatial variability of soil properties and relying solely on the mean values of material parameters for deterministic analysis will be more likely to underestimate the subsurface settlement.

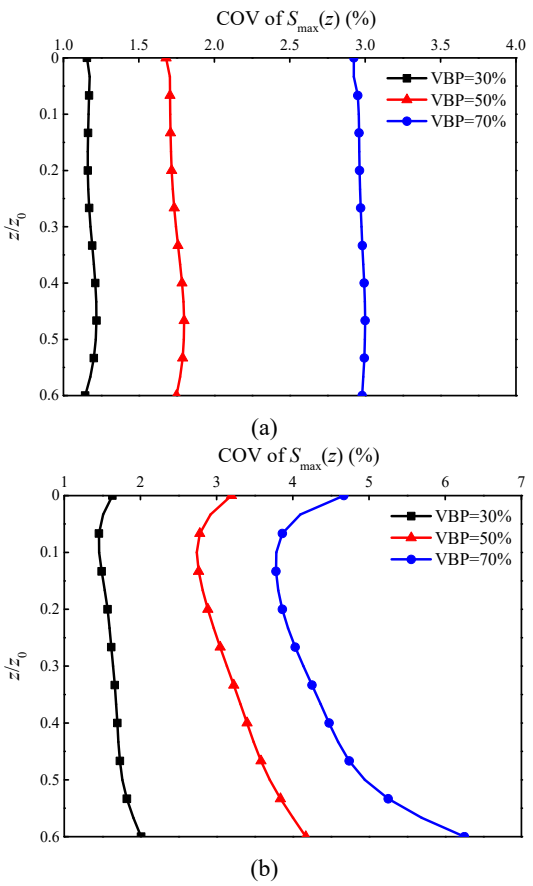


**Fig. 9 COV of stochastic analysis results for subsurface maximum settlement: (a)$\eta_t$ = 0.5%; (b) $\eta_t$ = 4.0%**

The variation of the COV of the stochastic analysis results with depth is shown in Fig. 9. Regardless of $\eta_t$, the COV at the same depth increases with increasing VBP, and the COV for the case of higher $\eta_t$ is always greater than that of lower $\eta_t$. When $\eta_t$ = 0.5%, the COVs for the same VBP but at different depths are not significantly different, and the COV does not change much with depth. Whereas, when $\eta_t$ = 4.0%, the COVs for the same VBP but at different depths vary more significantly; as the depth increases, the COV first decreases and then increases, with a greater change in amplitude as the VBP increases.

### 3.2.3 Subsurface soil volume loss rate

For tunnelling in drained soil (e.g., sandy cobble strata), the volumetric deformation (i.e., contraction or dilation) of the soil occurs due to shear, meaning that soil volume loss rate $\eta_s(z)$ varies with depth $z$ and is not equal to the tunnel volume loss rate $\eta_t$. According to the localized response of volumetric deformation, Wang et al. (2024) proposed three volumetric deformation modes of sandy cobble soil, as shown in Fig. S3 of the ESM. Fig. 10 compares the results of stochastic and deterministic analyses of the normalized ground loss rate with depth when $\eta_t$ = 0.5% and 4.0%. Overall, the soil above the tunnel crown tends to have a more dilative (less contractive) volumetric deformation response for the case of higher VBP or higher $\eta_t$. Conversely, the case with lower VBP or lower $\eta_t$ tends to evoke a more contractive (less dilative) response. These results are consistent with the deterministic analysis results.

Furthermore, although the mean of the stochastic analysis results does not differ significantly from that of the deterministic analysis results (that is, the volumetric deformation mode of the soil obtained from the mean of stochastic analysis results is consistent with that from the deterministic analysis), from a probabilistic perspective, there is still a certain probability that the stochastic analysis results may yield a different volumetric deformation mode. As shown in Fig. 10c, both the deterministic analysis results and the mean of the stochastic analysis results indicate that the volumetric deformation mode of the soil above the tunnel crown should belong to mode $II_1$. Only a small region of the soil close to the tunnel crown has a considerable localized dilative response, while the rest of the soil has a localized contractive response. The overall response of the soil close to the tunnel crown is dilative, while the rest of the soil has an overall contractive response. However, in Fig. 10c, for some of the stochastic analysis results, both the overall and localized volumetric deformation responses of the soil are contractive at any depth, indicating that the volumetric deformation mode of the soil should belong to mode I. Therefore, neglecting the spatial variability of soil properties and relying solely on the mean values of material pa-

rameters for deterministic analysis may not be sufficient to accurately assess the volumetric deformation mode of the soil above the tunnel crown, potentially affecting the prediction of subsurface settlement.

The variation of the COV of the stochastic analysis results with depth is shown in Fig. 11. Regardless of $\eta_t$, the COV at the same depth always increases with the increase of VBP, and the COV for the case of higher $\eta_t$ is always greater than that of lower $\eta_t$. When $\eta_t$ = 0.5%, the COVs for the same VBP increases with depth. Whereas, when $\eta_t$ = 4.0%, as the depth increases, the COVs for the same VBP first decrease then increase, and then continues to decrease with a relatively small magnitude.

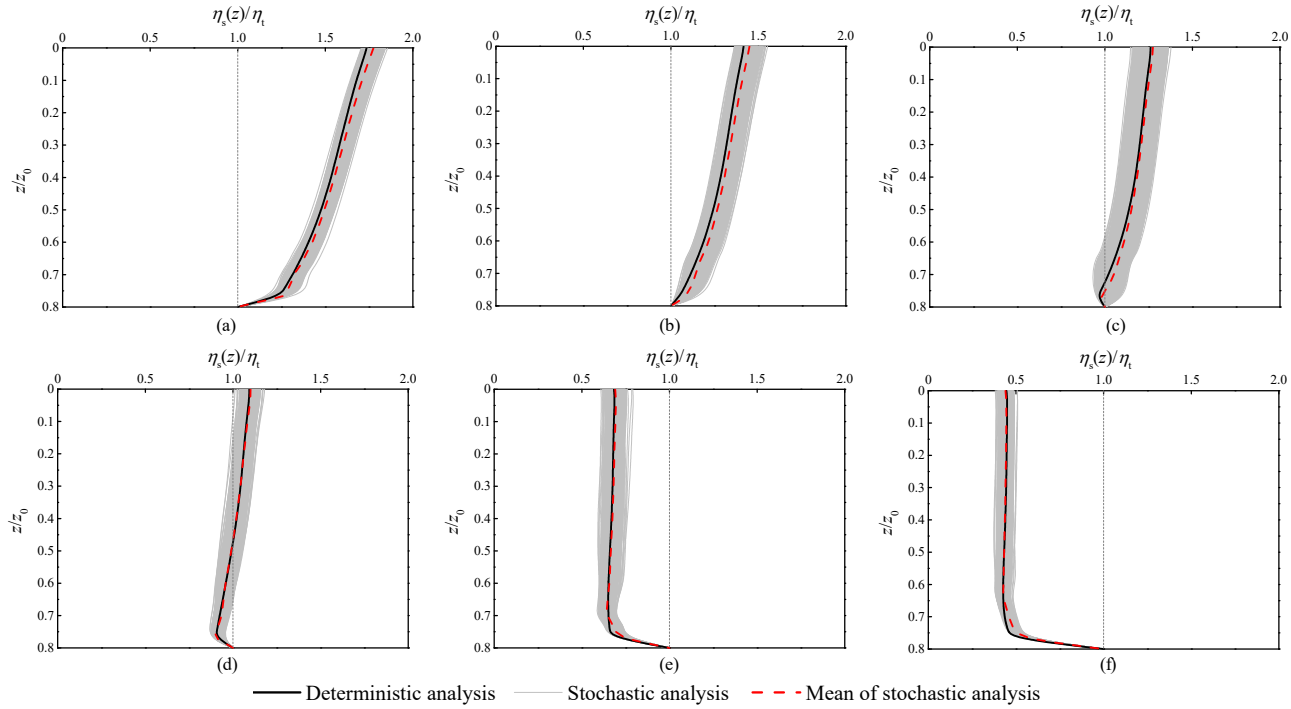


**Fig. 10 Comparison of normalized subsurface soil volume loss rate between stochastic analysis and deterministic analysis: (a)VBP = 30%, $\eta_t$ = 0.5%; (b) VBP = 50%, $\eta_t$ = 0.5%; (c) VBP = 70%, $\eta_t$ = 0.5%; (d) VBP = 30%, $\eta_t$ = 4.0%; (e) VBP = 50%, $\eta_t$ = 4.0%; (f) VBP = 70%, $\eta_t$ = 4.0%**

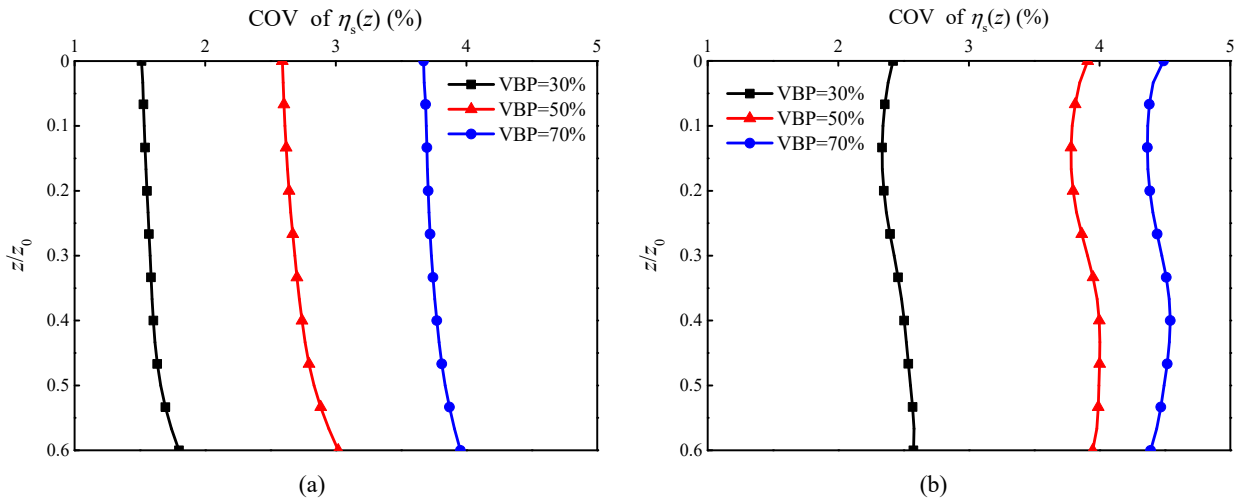


**Fig. 11 COV of stochastic analysis results for subsurface soil volume loss rate: (a) $\eta_t$ = 0.5%; (b) $\eta_t$ = 4.0%**

## 4 Discussion

The key input parameters in a random field, such as the COV, horizontal and vertical scales of fluctuation ($\delta_h$ and $\delta_v$) and cross-correlation coefficient of material parameters ($\rho$), are generally obtained based on statistical analysis of a large amount of field measurement data. However, in geotechnical engineering, the available field measurement data are often limited and insufficient to obtain accurate values of each input parameter. Therefore, considering the spatial variability of the reference stiffness modulus ($E_{50}^{ref}$) and friction angle ($\varphi$) of sandy cobble soil, this section discussed the impacts of the key input parameters in a random field ($COV_E$, $COV_\varphi$, $\delta_h$, $\delta_v$, and $\rho_{\varphi,E}$) on the stochastic analysis results of ground settlement. The values of the input parameters in the random field are shown in Table 1. Here, only the case of VBP = 50% and $\eta_t$ = 2.0% was considered. When discussing the effect of an input parameter, other parameters were kept constant at their values indicated in bold in Table 1.

### 4.1 Effect of $COV_\varphi$

The effect of $COV_\varphi$ on the variation of the COV of the stochastic analysis results for subsurface maximum settlement $S_{max}(z)$ and soil volume loss rate $\eta_s(z)$ with depth is depicted in Fig. 12. As the $COV_\varphi$ increases, both the COVs of $S_{max}(z)$ and $\eta_s(z)$ at the same depth significantly increase. For the case of lower $COV_\varphi$, both the COVs of $S_{max}(z)$ and $\eta_s(z)$ do not vary much with depth. Whereas, as the $COV_\varphi$ increases, the variation of the COVs with depth becomes more noticeable. Additionally, as the depth increases, both the COVs of $S_{max}(z)$ and $\eta_s(z)$ slightly decrease near the ground surface and then gradually increase.

For the mean of the normalized subsurface maximum settlement, as shown in Fig. S4a of the ESM, the mean value increases gradually with depth, and the mean value at the same depth slightly decreases as the $COV_\varphi$ increases. In Fig. S4b of the ESM, the mean value of the normalized subsurface soil volume loss rate does not differ significantly, and the corresponding volumetric deformation modes of the soil are all mode $II_2$, which is the same as the deterministic analysis result.

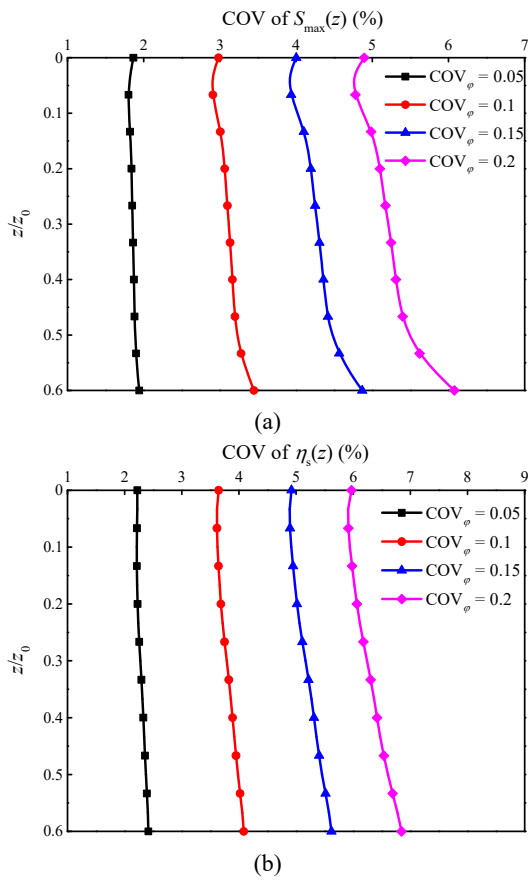


**Fig. 12 COV of stochastic analysis results under different $COV_\varphi$: (a) Subsurface maximum settlement; (b) Subsurface soil volume loss rate**

### 4.2 Effect of $COV_E$

The effect of $COV_E$ on the variation of the mean and COV of the stochastic analysis results for subsurface maximum settlement $S_{max}(z)$ with depth is shown in Fig. S5a of the ESM and Fig. 13a. The mean value of $S_{max}(z)$ at the same depth increases slightly with the increase of $COV_E$, while the COV of $S_{max}(z)$ at the same depth increases significantly. Overall, except for depths near the ground surface and near the tunnel crown, the COVs of $S_{max}(z)$ at different depths do not vary much. Comparing Figs. 12a and 13a, tunnelling-induced ground settlement is more sensitive to the variability of the internal friction angle than that of the reference secant modulus. This finding aligns with the result reported by Li et al. (2019). The reason may be that the internal friction angle, a critical parameter for assessing soil shear strength, is directly related to the shear capacity of soil and the development of plastic zones. The variability of the

reference secant modulus can influence the magnitude of soil deformation, but this effect is generally not as critical as that of the internal friction angle.

Fig. S5b in the ESM and Fig. 13b depict the effect of $COV_E$ on the variation of the mean and COV of the stochastic analysis results for soil volume loss rate $\eta_s(z)$ with depth, respectively. The mean values of the stochastic analysis results under different $COV_E$ do not differ significantly and the corresponding volumetric deformation modes of the soil are all mode $II_2$. Moreover, as the $COV_E$ increases, the volumetric deformation mode of the soil tends more towards mode $II_1$. The COV of $\eta_s(z)$ changes slightly with depth. Additionally, the COV of $\eta_s(z)$ at the same depth increases significantly as the $COV_E$ increases.

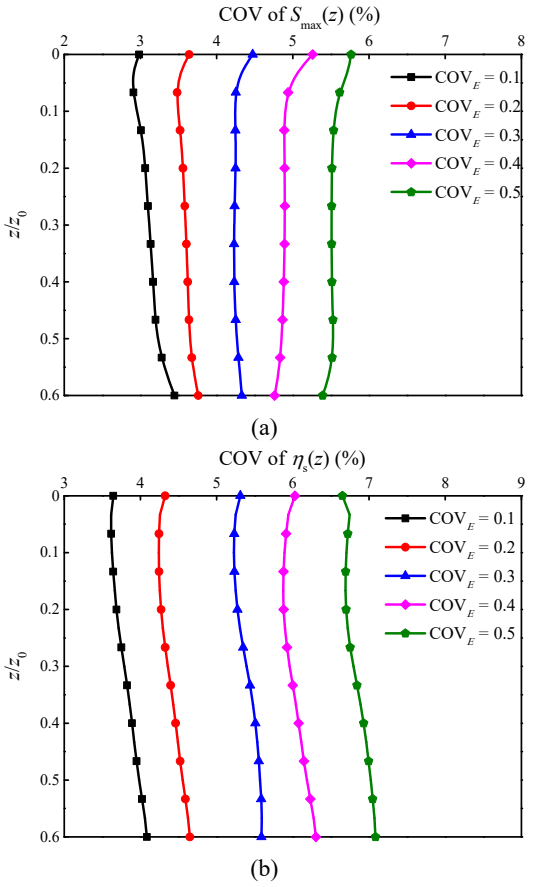


**Fig. 13 COV of stochastic analysis results under different $COV_E$: (a) Subsurface maximum settlement; (b) Subsurface soil volume loss rate**

## 4.3 Effect of $\delta_h$

The effect of $\delta_h$ on the variation of the COV of the stochastic analysis results for subsurface maximum settlement $S_{max}(z)$ and soil volume loss rate $\eta_s(z)$ with depth is depicted in Fig. 14. Both the COVs of $S_{max}(z)$ and $\eta_s(z)$ at the same depth increase gradually with the increase of $\delta_h$; after the $\delta_h$ reaches 30 m (five times the tunnel diameter), the COV no longer increases significantly but fluctuates within a small range. Moreover, as the depth increases, the COV of $S_{max}(z)$ slightly decreases near the ground surface and then continues to increase gradually, while the COV of $\eta_s(z)$ continues to increase gradually.

The variation of the mean for normalized subsurface maximum settlement and soil volume loss rate with depth under different $\delta_h$ is shown in Fig. S6 of the ESM. The $\delta_h$ has a negligible effect on the mean value of the stochastic analysis results and can be disregarded. All the volumetric deformation modes of the soil belong to mode $II_2$ (Fig. S6b).

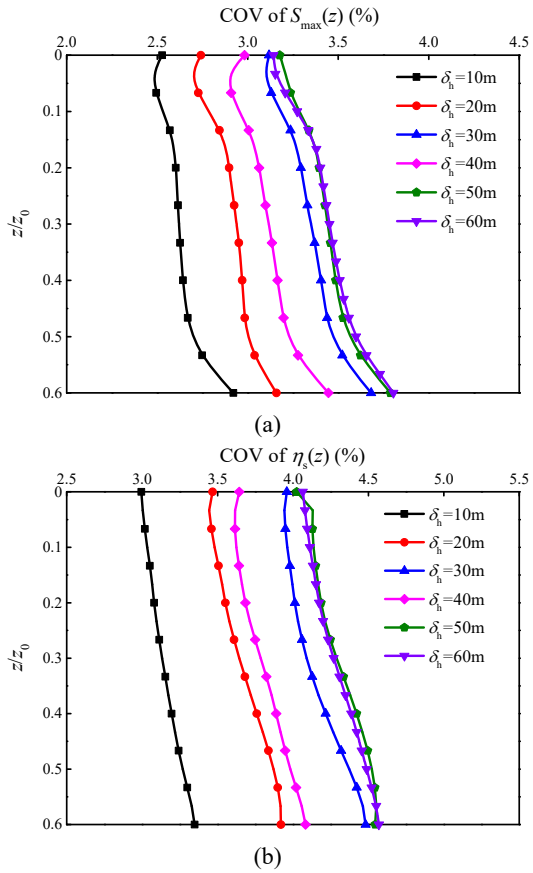


**Fig. 14 COV of stochastic analysis results under different $\delta_h$: (a) Subsurface maximum settlement; (b) Subsurface soil volume loss rate**

## 4.4 Effect of $\delta_v$

As shown in Fig. S7 of the ESM, the mean values of both $S_{max}(z)$ and $\eta_s(z)$ are almost unaffected by the $\delta_v$, and all the corresponding volumetric deformation modes of the soil are mode $II_2$. Fig. 15 presents the effect of $\delta_v$ on the variation of the COVs for $S_{max}(z)$ and $\eta_s(z)$ with depth. The COVs of $S_{max}(z)$ and $\eta_s(z)$ at the same depth significantly increase with the increase of $\delta_v$. In addition, as the depth increases, the COVs of $S_{max}(z)$ and $\eta_s(z)$ decrease slightly near the ground surface and then gradually increase, but the magnitude of change is not significant.

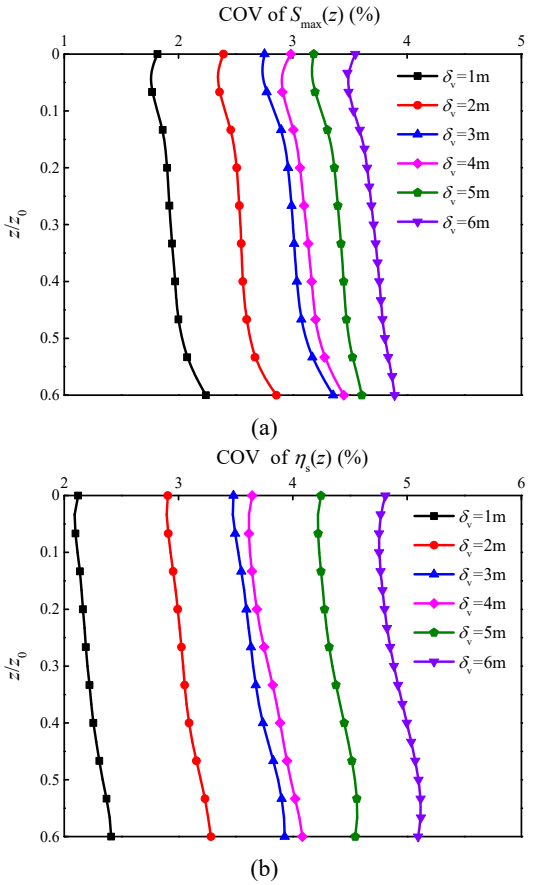


**Fig. 15 COV of stochastic analysis results under different $\delta_v$: (a) Subsurface maximum settlement; (b) Subsurface soil volume loss rate**

Fig. 16 illustrates the effects of $\delta_h$ and $\delta_v$ on the probability of maximum surface settlements exceeding the allowable values ($S_{max} > S_{max}^*$). There is only a minor difference among the cumulative probability distribution curves under different $\delta_h$, whereas there is a more significant difference among those under different $\delta_v$. This indicates that the vertical scale of fluctuation $\delta_v$ has a more pronounced effect on the probabilistic characteristics of surface settlement than the horizontal scale of fluctuation $\delta_h$.

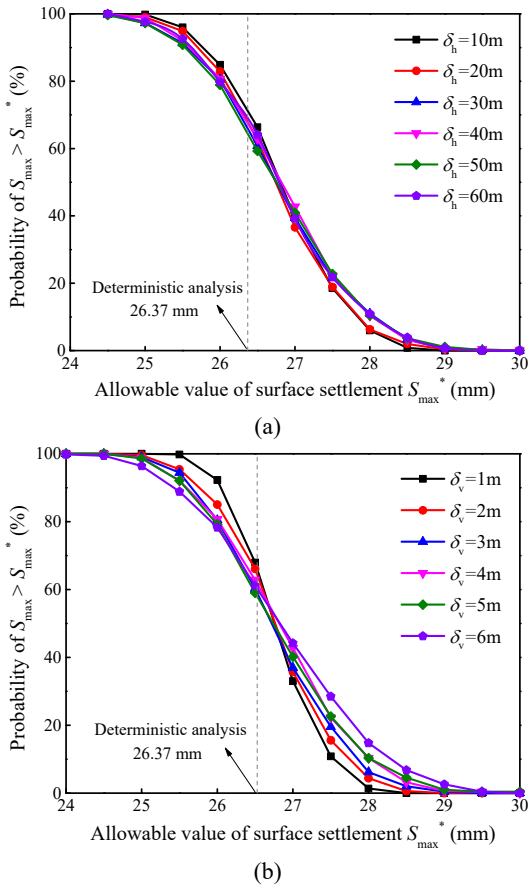


**Fig. 16 Effects of $\delta_h$ and $\delta_v$ on the probability of maximum surface settlements exceeding the allowable values: (a) $\delta_h$; (b) $\delta_v$**

## 4.5 Effect of $\rho_{\varphi,E}$

Engineering experience suggests that the internal friction angle tends to exhibit a positive correlation with the reference secant modulus. Fig. S8 in the ESM and Fig. 17 present the effect of $\rho_{\varphi,E}$ on the variation of the mean and COV of the stochastic analysis results for subsurface maximum settlement $S_{max}(z)$ and soil volume loss rate $\eta_s(z)$ with depth. The mean values of both $S_{max}(z)$ and $\eta_s(z)$ are almost unaffected by the $\rho_{\varphi,E}$, while the COVs of both $S_{max}(z)$ and $\eta_s(z)$ at the same depth decrease with the increase of $\rho_{\varphi,E}$. However, the variation of $\rho_{\varphi,E}$ has a relatively minor impact on the COVs of $S_{max}(z)$ and $\eta_s(z)$. The reason may be that the internal friction angle and reference secant modulus characterize different me-

chanical properties of sandy cobble soil. The internal friction angle indicates the shear strength of the soil, while the reference secant modulus indicates the stiffness or deformation characteristics, exhibiting relative independence in their physical significance. Even if there is a certain correlation between the two parameters, the effect of the correlation on ground settlement may be overshadowed by the high sensitivity to the internal friction angle. In addition, as the depth increases, the COVs of $S_{\max}(z)$ and $\eta_s(z)$ decrease slightly near the ground surface and then gradually increase, but the magnitude of change is not significant.

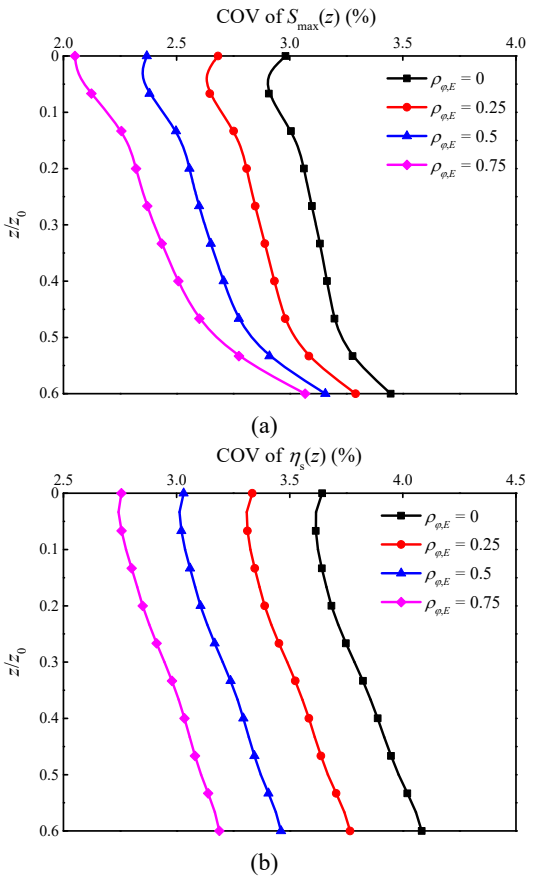


**Fig. 17 COV of stochastic analysis results under different $\rho_{\varphi,E}$: (a) Subsurface maximum settlement; (b) Subsurface soil volume loss rate**

## 5 Conclusions

Considering the spatial variability of the internal friction angle and reference secant modulus of sandy cobble soil, this paper employed the non-intrusive random finite difference method to investigate the probabilistic characteristics of surface and subsurface settlements induced by volume loss of shield tunnels based on random field theory and Monte Carlo simulation strategy. The main conclusions are as follows.

(1) The volumetric block proportion (VBP) and tunnel volume loss rate ($\eta_t$) have significant effects on the dispersion of the stochastic analysis results for settlement characteristics. The higher the VBP or the greater the $\eta_t$, the higher the dispersion of the stochastic analysis results. Moreover, the lower the VBP or the lower the $\eta_t$, the higher the probability of the stochastic analysis results exceeding the deterministic analysis results. In this case, it the surface and subsurface settlements are more likely to be underestimated if deterministic analysis is conducted using only the mean values of material parameters and neglecting the spatial variability of soil properties.

(2) Variation in the mean value of the stochastic analysis results for soil volume loss rate with depth generally exhibits no significant deviation from the deterministic analysis results. Specifically, the volumetric deformation mode of the soil derived from the average of stochastic analysis outcomes aligns consistently with that obtained through deterministic analysis. However, from a probabilistic perspective, there is still a certain probability that the stochastic analysis results may yield a volumetric deformation mode different from that of the deterministic analysis. Therefore, neglecting the spatial variability of soil properties and relying solely on the mean values of material parameters for deterministic analysis may be insufficient to accurately assess the volumetric deformation mode of the soil above the tunnel crown, potentially affecting the prediction of subsurface settlement.

(3) The mean value of the stochastic analysis results for settlement characteristics decreases slightly with the increase of $\mathrm{COV}_\varphi$, but increases slightly with the increase of $\mathrm{COV}_E$. Relatively speaking, the values of $\delta_h$, $\delta_v$, and $\rho_{\varphi,E}$ have a negligible impact on the mean value of the stochastic analysis results.

(4) The COV of the stochastic analysis results for settlement characteristics at the same depth increases with the increase of $\mathrm{COV}_\varphi$, $\mathrm{COV}_E$, and $\delta_v$. For the effect of $\delta_h$, the COV at the same depth increases gradually; after the $\delta_h$ reaches five times the tunnel

diameter, the COV no longer increases significantly but fluctuates within a small range. Moreover, the impact of $\delta_v$ on the probabilistic characteristics of ground settlements is more significant than that of $\delta_h$. Additionally, the COV at the same depth decreases with the increase of $\rho_{\varphi,E}$.

## Acknowledgments

The authors gratefully acknowledge the financial support provided by the Natural Science Foundation of Beijing Municipality (No. 8222004), the National Natural Science Foundation of China (No. 51978019), Doctoral Research Initiation Fund of Henan University of Science and Technology (No. 4007/13480062) and the Joint Fund of Science and Technology R&D Program of Henan, China (No. 232103810082).

## Author contributions

All authors contributed to the conception of the study. Fan WANG and Pengfei LI designed the research. Fan WANG processed the corresponding data and wrote the first draft of the manuscript. Pengfei LI revised and edited the final version. Xiuli DU provided the resources and supervised the manuscript process. Jianjun MA and Lin WANG helped organize the manuscript.

## Conflict of interest

Fan WANG, Pengfei LI, Xiuli DU, Jianjun MA, and Lin WANG declare that they have no conflict of interest.

## References

Ali A, Lyamin AV, Huang J, et al., 2017. Undrained stability of a single circular tunnel in spatially variable soil subjected to surcharge loading. *Computers and Geotechnics*, 84: 16–27. https://doi.org/10.1016/j.compgeo.2016.11.013

Cao S, Cui J, Fang Y, et al., 2019. Performance of slurry TBM tunnelling in sandy cobble ground — a case study in Lanzhou. *KSCE Journal of Civil Engineering*, 23: 3207–3217. https://doi.org/10.1007/s12205-019-1627-4

Chen D, Xu D, Ren G, et al., 2019. Simulation of cross-correlated non-Gaussian random fields for layered rock mass mechanical parameters. *Computers and Geotechnics*, 112: 104–119. https://doi.org/10.1016/j.compgeo.2019.04.012

Cheng H, Chen J, Chen R, et al., 2019. Reliability study on shield tunnel face using a random limit analysis method in multilayered soils. *Tunnelling and Underground Space Technology*, 84: 353–363. https://doi.org/10.1016/j.tust.2018.11.038

Cheng H, Chen J, Chen R, et al., 2019a. Comparison of modeling soil parameters using random variables and random fields in reliability analysis of tunnel face. *International Journal of Geomechnics*, 19: 1–13. https://doi.org/10.1061/(ASCE)GM.1943-5622.0001330

Cheng H, Chen J, Chen R, et al., 2019b. Three-dimensional analysis of tunnel face stability in spatially variable soils. *Computers and Geotechnics*, 111: 76–88. https://doi.org/10.1016/j.compgeo.2019.03.005

Cheng H, Chen J, Li J, 2019c. Probabilistic analysis of ground movements caused by tunneling in a spatially variable soil. *International Journal of Geomechnics*, 19: 1–10. https://doi.org/10.1061/(ASCE)GM.1943-5622.0001526

Ching J, Phoon KK, 2013. Effect of element sizes in random field finite element simulations of soil shear strength. *Computers and Structures*, 126: 120–134. https://doi.org/10.1016/j.compstruc.2012.11.008

Deng Z, Pan M, Niu J, et al., 2022. Full probability design of soil slopes considering both stratigraphic uncertainty and spatial variability of soil properties. *Bulletin of Engineering Geology and the Environment*, 81: 195. https://doi.org/10.1007/s10064-022-02702-2

Di Q, Li P, Zhang M, et al., 2022. Investigation of progressive settlement of sandy cobble strata for shield tunnels with different burial depths. *Engineeing Failure Analysis*, 141: 106708. https://doi.org/10.1016/j.engfailanal.2022.106708

Hao X, Sun Z, Zhao Y, et al., 2021. Characteristics of ground surface settlement of double-line adjacent metro construction in sandy cobble stratum: a case study of Beijing airport line. *KSCE Journal of Civil Engineering*, 25: 4443–4456. https://doi.org/10.1007/s12205-021-0057-2

He C, Feng K, Fang Y, et al., 2012. Surface settlement caused by twin-parallel shield tunnelling in sandy cobble strata. *Journal of Zhejiang University-Science A*, 13: 858–869. https://doi.org/10.1631/jzus.A12ISGT6

Huang HW, Xiao L, Zhang DM, et al., 2017. Influence of spatial variability of soil Young's modulus on tunnel convergence in soft soils. *Engineering Geology*, 228: 357–370. https://doi.org/10.1016/j.enggeo.2017.09.011

Huang SP, Quek ST, Phoon KK, 2001. Convergence study of the truncated Karhunen–Loeve expansion for simulation of stochastic processes. *International Journal for Numerical Methods in Engineering*, 52: 1029–1043. https://doi.org/10.1002/nme.255

Itasca, 2017. FLAC$^{3D}$—Fast Lagrangian Analysis of Continua in 3 Dimensions. Version 6.0. Itasca, Minneapolis.

Jiang SH, Li DQ, Zhang LM, et al., 2014. Slope reliability analysis considering spatially variable shear strength parameters using a non-intrusive stochastic finite element method. *Engineering Geology*, 168: 120–128. https://doi.org/10.1016/j.enggeo.2013.11.006

Jiang SH, Huang J, Griffiths DV, et al., 2022. Advances in reliability and risk analyses of slopes in spatially variable soils: a state-of-the-art review. *Computers and Geotechnics*, 141: 104498. https://doi.org/10.1016/j.compgeo.2021.104498

Li DQ, Jiang SH, Cao ZJ, et al., 2015. A multiple response-surface method for slope reliability analysis con-

sidering spatial variability of soil properties. *Engineering Geology*, 187: 60–72.
https://doi.org/10.1016/j.enggeo.2014.12.003

Li J, Chen J, Cheng H, et al., 2019. Sensitivity analysis of mechanical parameters to surrounding-soil response induced by shield tunneling considering spatial variability. *Chinese Journal of Rock Mechanics and Engineering*, 38(8): 1667-1676 (in Chinese).

Li T, Gong W, Tang H, 2021. Three-dimensional stochastic geological modeling for probabilistic stability analysis of a circular tunnel face. *Tunnelling and Underground Space Technology*, 118: 104190.
https://doi.org/10.1016/j.tust.2021.104190

Li T, Pan Q, Shen Z, et al., 2022. Probabilistic Stability Analysis of a Tunnel Face in Spatially Random Hoek–Brown Rock Masses with a Multi-Tangent Method. *Rock Mechnics and Rock Engineering*, 55: 3545–3561.
https://doi.org/10.1007/s00603-022-02821-y

Li, X, Geng A, 2024. Investigation and measurement of old building response to the overlapped shield tunnel of multiple schemes in the sandy cobble stratum. *Underground Space*, 15: 260–274.
https://doi.org/10.1016/j.undsp.2023.08.016

Lü Q, Xiao Z, Zheng J, et al., 2018. Probabilistic assessment of tunnel convergence considering spatial variability in rock mass properties using interpolated autocorrelation and response surface method. *Geoscience Frontiers*, 9: 1619–1629.
https://doi.org/10.1016/j.gsf.2017.08.007

Mollon G, Dias D, Soubra AH, 2011. Probabilistic analysis of pressurized tunnels against face stability using collocation-based stochastic response surface method. *Journal of Geotechnical and Geoenvironmental Engineering*, 137: 385–397.
https://doi.org/10.1061/(ASCE)GT.1943-5606.0000443

Mollon G, Dias D, Soubra A, et al., 2009a. Probabilistic analysis and design of circular tunnels against face stability. *International Journal of Geomechnics*, 9: 237–249.
https://doi.org/10.1061/(ASCE)1532-3641(2009)9:6(237
)

Mollon G, Dias D, Soubra A., et al., 2009b. Probabilistic Analysis of Circular Tunnels in Homogeneous Soil Using Response Surface Methodology. *Journal of Geotechnical and Geoenvironmental Engineering*, 135: 1314–1325.
https://doi.org/10.1061/(ASCE)GT.1943-5606.0000060

Mollon G, Dias D, Soubra AH, 2013. Probabilistic analyses of tunneling-induced ground movements. *Acta Geotechnica*, 8: 181–199.
https://doi.org/10.1007/s11440-012-0182-7

Pan Q, Dias D, 2017. Probabilistic evaluation of tunnel face stability in spatially random soils using sparse polynomial chaos expansion with global sensitivity analysis. *Acta Geotechnica*, 12: 1415–1429.
https://doi.org/10.1007/s11440-017-0541-5

Pan Y, Yao K, Phoon KK, et al., 2019. Analysis of tunnelling through spatially-variable improved surrounding – A simplified approach. *Tunnelling and Underground Space Technology*, 93: 103102.
https://doi.org/10.1016/j.tust.2019.103102

Pandit B, Sivakumar Babu GL, 2021. Probabilistic stability assessment of tunnel-support system considering spatial variability in weak rock mass. *Computers and Geotechnics*, 137: 104242.
https://doi.org/10.1016/j.compgeo.2021.104242

Schanz T, Vermeer PA, Bonnier PG, 1999. The hardening soil model: Formulation and verification. Beyond 2000 in computational geotechnics. Ten Years of PLAXIS International. Proceedings of the international symposium, Amsterdam, p. 281–296.
https://doi.org/10.1201/9781315138206-27

Vanmarcke EH, 1977. Probabilistic Modeling of Soil Profiles. *Journal of the Geotechnical Engineering Division*, 103: 1227–1246.
https://doi.org/10.1061/AJGEB6.0000517

Wang F, Du X, Li P, 2024. Prediction of subsurface settlement induced by shield tunnelling in sandy cobble stratum. *Journal of Rock Mechanics and Geotechnical Engineering*, 16: 192–212.
https://doi.org/10.1016/j.jrmge.2023.08.001

Wang F, Du X, Li P, 2023a. Predictions of ground surface settlement for shield tunnels in sandy cobble stratum based on stochastic medium theory and empirical formulas. *Underground Space*, 11: 189–203.
https://doi.org/10.1016/j.undsp.2023.01.003

Wang F, Du X, Li P, et al., 2023b. A meso-scale numerical modelling method for the stability analysis of tunnels in sandy cobble stratum. *Transportation Geotechnics*, 38: 100921.
https://doi.org/10.1016/j.trgeo.2022.100921

Wu G, Zhao H, Zhao M, et al., 2021. Stochastic analysis of dual tunnels in spatially random soil. *Computers and Geotechnics*, 129: 103861.
https://doi.org/10.1016/j.compgeo.2020.103861

Wu H, Gan X, Liu N, et al., 2024. Analysis of tunneling-induced ground movements in spatially variable soil under the influence of existing building. *Computers and Geotechnics*, 166: 106003.
https://doi.org/10.1016/j.compgeo.2023.106003

Wu Y, Bao H, Wang J, et al., 2021. Probabilistic analysis of tunnel convergence on spatially variable soil: The importance of distribution type of soil properties. *Tunnelling and Underground Space Technology*, 109: 103747.
https://doi.org/10.1016/j.tust.2020.103747

Zhang H, Luo F, Geng W, et al., 2023. An efficient method for reliability analysis of high-speed railway tunnel convergence in spatially variable soil based on a deep convolutional neural network. *International Journal of Geomechanics*, 23: 1–15.
https://doi.org/10.1061/IJGNAI.GMENG-8644

Zhang JZ, Huang HW, Zhang DM, et al., 2021. Effect of ground surface surcharge on deformational performance of tunnel in spatially variable soil. *Computers and Geotechnics*, 136: 104229.

https://doi.org/10.1016/j.compgeo.2021.104229
Zhang S, Wang Y, Gao Q, et al., 2024. Probabilistic analysis of ground settlement induced by tunnel excavation in multilayered soil considering spatial variability. *Computers and Geotechnics*, 165: 105951. https://doi.org/10.1016/j.compgeo.2023.105951
Zhang W, Han L, Gu X, et al., 2022. Tunneling and deep excavations in spatially variable soil and rock masses: A short review. *Underground Space*, 7: 380–407. https://doi.org/10.1016/j.undsp.2020.03.003
Zhang ZX, Liu C, Huang X, et al., 2016. Three-dimensional finite-element analysis on ground responses during twin-tunnel construction using the URUP method. *Tunnelling and Underground Space Technology*, 58: 133–146. https://doi.org/10.1016/j.tust.2016.05.001

## Electronic supplementary materials

Sections S1–S6, Figs. S1–S8, Table S1

# 中文概要

**题　目：考虑空间变异性的砂卵石地层盾构隧道沉降特征概率分析**

**作　者：**王帆[1]，李鹏飞[2]，杜修力[2]，马建军[1]，王林[1]
**机　构：**[1]河南科技大学，土木建筑学院，中国洛阳，471023；[2]北京工业大学，城市与工程安全减灾教育部重点实验室，中国北京，100124

**目　的：**砂卵石地层具有显著非均质性和随机性特点，在进行地层沉降研究时，有必要考虑土性参数空间变异性。本文旨在探讨不同含石量与不同隧道体积损失率情况下砂卵石地层盾构隧道施工诱发地表和地中沉降的概率统计特征。

**创新点：**1. 考虑土性参数空间变异性，对比分析了砂卵石地层盾构隧道沉降特征的确定性分析结果与随机分析结果；2. 讨论了随机场输入参数对地层沉降概率统计特征的影响。

**方　法：**考虑内摩擦角和参考割线模量的空间变异性，基于非侵入式随机有限差分法和蒙特卡罗模拟策略，研究了砂卵石地层盾构隧道地表最大沉降、地中沉降槽宽度、地中最大沉降和地中地层损失率的概率统计特征。

**结　论：**1. 地层含石量或隧道体积损失率越大，地层沉降随机分析结果离散性越高；2. 忽略土性参数空间变异性而仅采用参数均值进行确定性分析，有可能低估地层沉降；3. 地层沉降随机分析结果的变异系数随着土性参数变异系数和波动范围的增大而增大，但随着内摩擦角与参考割线模量互相关系数的增大而减小。

**关键词：**盾构隧道；砂卵石地层；沉降特征；空间变异性；概率分析